Influence of the reactor configuration and the supporting electrolyte concentration on the electrochemical oxidation of Atenolol using BDD and SnO_2 ceramic electrodes.

J. Mora-Gómez[a], M. García-Gabaldón[a*], J. Carrillo-Abad[a], M. T. Montañés[a], S. Mestre[b], V. Pérez-Herranz[a]

[a]IEC Group, ISIRYM, Universitat Politècnica de València, Camí de Vera s/n, 46022, València, P.O. Box 22012, E-46071, Spain

[b]Instituto Universitario de Tecnología Cerámica, Universitat Jaume I, Castellón, Spain.

*Corresponding author: mongarga@iqn.upv.es

Abstract

Electrochemical oxidation of β-blocker atenolol (ATL, 100 ppm) at different applied current densities (33, 50 and 83 $mA \cdot cm^{-2}$) using a reactor divided by an ion-exchange membrane and an undivided one was investigated. Two types of anodes were used for this purpose: a boron-doped diamond (BDD) anode and new low-cost ceramic electrodes made of tin dioxide doped with antimony (Sb-doped SnO_2). Degradation was assessed using a high performance liquid chromatography, while mineralization by measuring total organic carbon (TOC) dissolved in sample. Except for the lowest current density, ATL was completely

degraded for both reactors and electrodes. The highest percentage of TOC eliminated (89%) was obtained at the highest applied current density with the BDD electrode in the divided reactor. The presence of the cation-exchange membrane prevented the reduction of both the electrogenerated oxidizing species and the oxidized organic compounds and enhances the electro-oxidation kinetic reaction.

In order to study the influence of the supporting electrolyte, three different concentrations of sodium sulfate (0.014, 0.05 and 0.1 M) were tested in the undivided reactor with both electrodes. The results showed that an increase in the concentration of the supporting electrolyte improves the mineralization of ATL for the BDD electrode and, on the contrary, worsens for the ceramic electrode. Accelerated service life tests were carried out for the ceramic electrode at 100 $mA \cdot cm^{-2}$ in 0.5 M H_2SO_4. Ecotoxicity tests using marine bacteria (*Vibrio Fischeri*) revealed that no toxic by-products were formed in any case.

Keywords: Atenolol, BDD anode, electrochemical oxidation, Sb-doped SnO_2 ceramic anode, accelerated service life test, toxicity.

1. Introduction

The continuous introduction of pharmaceutical and personal care products (PPCPs) to the environment and the increasingly restrictive legislation, make PPCPs be considered emerging contaminants. Many of these compounds are not removed in conventional wastewater treatment plants (WWTPs) and pass into the environment [1–3]. This can suppose a significant risk to the health of the ecosystem.

For this reason, in recent years, many efforts are being dedicated to the investigation of different processes for the elimination of these emerging compounds. Advanced oxidation processes (AOPs) are attractive methods as a solution to this problem, specifically, the electrochemical advanced oxidation processes (EAOPs) [4–7] due to their low cost, high effectiveness and their kindness to the environment, since no chemical additives are used. In the group of EAOPs, one of the most prominent technique is the anodic oxidation. This technique is based on the destruction of the contaminant by: (i) direct oxidation, i.e. transfer of electrons from the compound to the anode or (ii) indirect oxidation by electrogenerated species on the surface of the anode, such as hydroxyl radicals ($^{\bullet}OH$):

$$M + H_2O \rightarrow M(^{\bullet}OH) + H^+ + e^- \quad (1)$$

where M is the anodic surface and M(•OH) the hydroxyl radicals sorbed on the anodic surface. However, undesirable reactions that consume these radicals and benefit the formation of oxygen can occur:

$$M(^{\bullet}OH) + H_2O \rightarrow M + O_2 + 3H^+ + 3e^- \quad (2)$$

$$2M(^{\bullet}OH) \rightarrow 2M + O_2 + 2H^+ + 2e^- \quad (3)$$

To avoid these reactions, the anode must possess a high overpotential towards the formation of O_2. In this sense, there are two types of anodes [5]: non-active and active ones, whose main difference is based on whether the hydroxyl radicals are physisorbed or chemisorbed on the surface. In the latter case, the radicals are oxidized and a covalent bond of oxygen with the metal is formed according to Equation 4:

$$M(^{\bullet}OH) \rightarrow MO + H^+ + e^- \quad (4)$$

Active anodes, such as Pt [8], graphite [9] and dimensionally stable anode (DSA) [10], are efficient for the oxidation of short-chain molecules, but not for complex molecules. In contrast, physisorbed radicals (non-active anodes) have a greater oxidant power and they are capable of mineralizing complex molecules to CO_2 and H_2O. As an example of these electrodes are boron-doped diamond (BDD) and oxides of Sn and Pb [11,12].

Nowadays, one of the most efficient anode is the BDD electrode [11,13]. This electrode has a high reactivity, a great oxygen overpotential and a high chemical stability. However, it is not viable on an industrial scale due to its high cost and its difficulty in the manufacture.

As an alternative, ceramic electrodes capable of competing with the BDD are being developed [14,15]. The advantages offered by the ceramic electrodes are their low cost, the increased active area due to its porosity, and the easiness of manufacture. In a previous study [16], new ceramic electrodes composed of SnO_2 doped with Sb were studied for the electrooxidation of the antibiotic Norfloxacin. In that study, it was found that this emerging compound could be effectively oxidized by these new electrodes. In every case, the electro-oxidation efficiency is considerably increased by means the use of an electrochemical reactor separated by an ion-exchange membrane, since the reduction reactions of the oxidant species and the intermediate compounds generated on the anode are avoided. Besides, with this reactor configuration, the more acidic pH reached in the anodic compartment enhances the electro-oxidation of the organic compounds of interest [16–18].

In this paper, the electrochemical study of these new ceramic electrodes for the degradation of another pharmaceutical compound recently found in the effluents of WWTPs, Atenolol (ATL), is carried out. ATL is a drug belonging to the group of beta-blockers used for the treatment of cardiovascular diseases such as hypertension, coronary heart diseases, arrhythmia, and myocardial infarction

after the acute event. In patients is practically eliminated by the kidneys. The problem related to this compound is the low elimination rate in WWWTPs [19].

A lot of studies have recently been carried out using the photocatalysis technique to remove ATL, in which the addition of a catalyst is necessary [20–22]. Several investigations have been conducted on the removal of Atenolol by electro-oxidation. Sirés et al. [23] studied the anodic oxidation of ATL using BDD and Pt as anodes at constant current at a pH of 3. They proved that BDD electrode is more effective than the Pt one due to the great amount of active $^{\bullet}OH$ generated on the surface of BDD, and the minimization of the parasitic reactions. Murugananthan et al. [24] compared different supporting electrolytes (Na_2SO_4, NaCl and $NaNO_3$) for the degradation of ATL with BDD and Pt electrodes. They showed that the worst electrolyte for the mineralization was $NaNO_3$, and the best conditions were obtained with the BDD electrode in Na_2SO_4 medium.

The objective of this work is to study the electrochemical oxidation of ATL with the new ceramic electrodes and thus prove their versatility for the removal of different compounds. Moreover, the influence of the reactor configuration (one-compartment and two-compartment reactor in the presence of a cation-exchange membrane) on the ATL electro-oxidation has also been evaluated. Under all the experimental conditions texted, the toxicity of the solutions submitted to the electro-oxidation is evaluated by *Vibrio fisheri* bacteria.

2. Experimental

2.1 Stability of the new Sb-doped SnO_2 ceramic electrodes

Electrodes based on SnO_2 doped with Sb present good characteristics to be used as anodes in EAOPs. However, their low stability to anodic polarization in aqueous media limits their use [25,26]. In this work, accelerated service life tests were carried out in 0.5 M H_2SO_4 solution at 100 $mA \cdot cm^{-2}$, considering that the electrode was deactivated when the potential overcomes 5 V from its initial value [27,28]. The tests were performed in a conventional three electrode cell, where the working electrode was the new Sb-SnO_2 ceramic electrode, and as counter and reference electrodes a Pt and an Ag/AgCl, encapsulated with 3 M KCl, electrodes were used, respectively.

2.2 Electrochemical oxidation

The electrochemical oxidation processes were carried out for a solution composed of 100 ppm Atenolol (ATL, Sigma-Aldrich) and 0.014M of Na_2SO_4 (Sigma-Aldrich) as supporting electrolyte. In order to study the effect of the supporting electrolyte, tests at different concentrations of Na_2SO_4 (0.014, 0.05 and 0.1 M) were also carried out.

The ATL molecule contains two reactive sites: the aromatic ring and the amino group. The first site does not depend on the solution pH, but the latter does. Atenolol is very hydrophilic and soluble in water, having a pK_a value of 9.6.

The divided reactor, whose schematic representations is shown in Figure 1, is formed by two glass chambers of 250 cm^3 each, separated by a Nafion 117 cation-exchange membrane (from Dupont) [16]. The membrane contact surface was 11.34 cm^2 and it was equilibrated with the working solution for 24 h before each experiment.

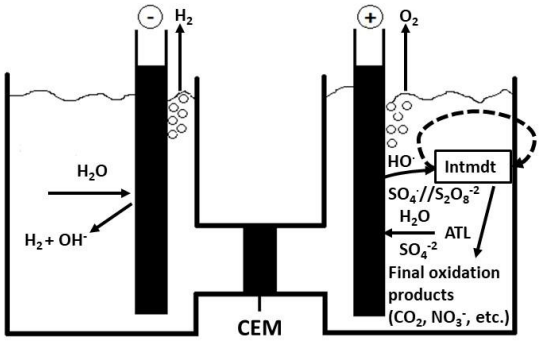

Figure 1. Schematic representation of the divided reactor and its main reactions.

250 cm^3 of the initial solution were introduced into the undivided reactor and in the anodic compartment of the divided reactor. The cathodic compartment was filled with the supporting electrolyte at the same concentration as that presented in the anolyte. The gap between cathode and anode was 6.5 and 1 cm for both undivided and divided reactors, respectively. Two types of working electrodes of similar contact surface (12 cm^2) were compared in this work: a Boron-doped diamond (BDD) film on a Niobium basis with a doping level of 2500 ppm purchased from NeoCoat SA (Switzerland), and the ceramic electrodes composed of Sb-doped SnO_2. The synthesis of these electrodes was also well described in previous works [15,16]. The raw materials (SnO_2 and Sb_2O_3 with a 98/2 molar ratio) were introduced into alumina jars with a planetary mill (Pulverisette 5, Fritsch GmbH, Germany). Then, this suspension was dried in a

furnace at 110 ° C during 24 hours. Specimens of 80 x 20 x 5 mm were obtained by pressing into an automatic press (Nanetti) that applied a force of 250 $kg \cdot cm^{-2}$. Finally, sintering process took place in a furnace (RHF1600, Carbolite Furnaces, UK), where the heating was at 5 $°C \cdot min^{-1}$ and the residence time was 1 hour to reduce the volatilization of antimony. The maximum sintering temperature was 1200 °C. The new ceramic electrodes presented an average apparent density of 3533±28 $Kg \cdot m^{-3}$, an electrical resistivity of 0.03901±0.00035 Ω·cm and a total pore volume of 0.133 $cm^3 \cdot g^{-1}$. The counter electrode consisted of a stainless-steel sheet (AISI 304) and the reference electrode was an Ag/AgCl electrode encapsulated with 3M KCl. All the tests were carried out in galvanostatic mode and at room temperature under stirring during 4 hours. The current densities studied for both reactors were 33, 50 and 83 $mA \cdot cm^{-2}$.

2.3 Analytical methods

2.3.1 Analysis of Atenolol mineralization

2 ml of sample solution were taken from the reactor for the measurement of ATL concentration, ATL mineralization and also for the ionic analysis. The evolution of the ATL concentration was monitored by measuring the samples extracted every 30 min using a high-performance liquid chromatograph (HPLC). The HPLC system was equipped with a PU-2089 quaternary gradient pump (Jasco, Japan), a Photodiode Array detector MD2018 Plus and a Kinetex XB-C18 column (100×4.6 mm, 5 µm, 100 Å). The operating conditions were: flow rate 1 $mL \cdot min^{-1}$,

injected volume 20.0 µL and wavelength UV detection at 224 nm. The elution was performed isocratically with methanol/water 15:85 (v/v) mixture as mobile phase.

The Total Organic Carbon (TOC) indicates the degree of mineralization achieved during the electrolytic process. The TOC values were obtained through a Shimadzu TNM-L ROHS TOC analyser. The method selected for these measurements was the non-purgeable organic carbon (NPOC), where the inorganic carbon is first removed by acidifying and then the organic one is measured. With the previous data, the percentages of TOC and ATL removed, and the extent of electrochemical combustion (Φ) [29,30] were calculated:

$$\emptyset = \frac{\%[TOC]_{removed}}{\%[ATL]_{removed}} \quad (5)$$

The mineralization current efficiency (MCE) defined as a function of the organic matter eliminated (Equation 6) [31,32], was also determined to quantify the efficiency of the process.

$$MCE(\%) = \frac{nFV\Delta(TOC)_t}{7.2 \cdot 10^5 mIt} \cdot 100 \quad (6)$$

where $\Delta[TOC]_t$ (mg·L^{-1}) is the removal of TOC after a certain time t(min), n is the number of exchanged electrons in the oxidation reaction, F is the Faraday constant (96485 C·mol^{-1}), V is the volume of the electrolytic cell (L), m is the number of carbon atoms in the ATL molecule (14), I the applied current (A) and $7.2x10^5$ is a conversion factor (60 s·min^{-1}x12000 mg·mol^{-1}). Assuming that all the nitrogen in the molecule passes to ammonium ions (NH_4^+), as explained in other

study [23], the number of exchanged electrons (n) was taken as 66 according to the following reaction:

$$C_{14}H_{22}N_2O_3 + 25H_20 \rightarrow 14CO_2 + 2NH_4^+ + 64H^+ + 66e^- \qquad (7)$$

Inorganic ions of nitrogen (NO_2^-, NO_3^- and NH_4^+) was monitored at the end of the electrolysis by a Metrohm Ionic Chromatograph equipped with a Metrosep A Supp 5-150/4.0 and a Metrosep C6-250/4.0, as anionic and cationic columns, respectively.

2.3.2 Iodometry tests

Iodometry tests were carried out to determine the total oxidants present in the samples. Specifically, in this study the oxidants may only be persulfates and hydrogen peroxide. The hydroxyl radicals cannot be determined by this method due to their low lifetime [33,34]. To carry out these tests, 2 grams of KI were added in the sample. The I^- ions reacted with the oxidants to form I_2 resulting in a yellow-orange solution.

The I_2 formed was titrated with 0.01 M sodium thiosulfate ($Na_2S_2O_3$) until the solution had a light-yellow colour. At this time a few drops of 1% starch (w/v) were added, and the solution turned dark brown-bluish coloured. Then, the titration was continued until the solution was transparent.

The concentration of H_2O_2 was determined using a colorimetric method [35]. And the difference between total oxidants and the amount of H_2O_2 generated was the amount of persulfates generated.

2.3.3 Toxicity measurements

In some cases, the oxidation process of the organic matter can lead to by-products more toxic than the initial compound [36,37]. Ecotoxicity tests were carried out by bioluminescence measurements of the *Vibrio Fischeri* bacterium to evaluate this phenomenon.

This study was carried out by the Microtox M-500 equipment (Microbics, 1989). The Microtox® system is a bioassay that examines the acute toxicity of environmental samples and pure compounds based on the reduction of the natural bioluminescence of the marine bacterium *Vibrio Fischeri* after 15 minutes of exposure at 15 °C [36]. Before each measurement, the samples were adjusted to a pH range between 6 and 8, with NaOH or H_2SO_4.

3. Results and discussion

3.1 Service life tests

Figure 2 shows the cell potential (V) evolution versus time (days) of the accelerated service life test at an applied current density of 100 $mA \cdot cm^{-2}$ in 0.5 M H_2SO_4 during 70 days. The initial value of cell potential was 3.7 V, and during the first hours of test this value increased up to 5 V. Then, the potential was increasing very slowly with time, showing practically no oscillations around this value.

The most common Sb-doped SnO_2 electrode used for EAOPs possess a titanium support (Ti/Sb-SnO_2) [25]. This electrode reached a lifetime of 12.1 h for the same conditions as those used in the present work [38].Comparing both results, it can be concluded that the ceramic substrate improves the stability of the electrodes based on SnO_2.

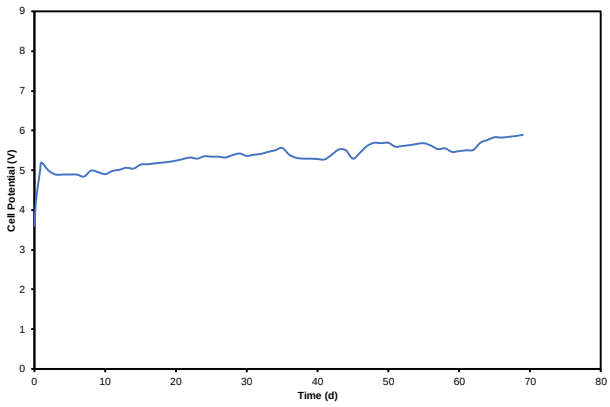

Figure 2. Accelerated service life curve of Sb-doped SnO_2 ceramic electrode in 0.5M H_2SO_4 at 100 $mA \cdot cm^{-2}$.

Different studies have been carried out with the aim of improving the service life of the most common Sb-doped SnO_2 electrodes. Xue et al. [39] studied the influence (at 500 $mA \cdot cm^{-2}$ and 1 M H_2SO_4) of the substrate structure, and found that the electrode with a porous substrate presented a higher lifetime in comparison with a planar one, having the values of 105 and 20 min, respectively. Another possible improvement is the incorporation of an interlayer. Correa-Lozano et al. [40] demonstrated that the addition of the IrO_2 interlayer increased the service life from 12 h to 900 h at a current density of 100 $mA \cdot cm^{-2}$ in 1 M H_2SO_4, while Shao et al. [26] prepared an electrode with a Titanium hydride interlayer that presented a lifetime of 72 h at 200 $mA \cdot cm^{-2}$ in 0.5 M H_2SO_4. The addition of metals can also improve the stability of this type of electrode. Zhuo et al. [28] doubled its lifetime (0.8 h, at 100 $mA \cdot cm^{-2}$ in 0.5 M H_2SO_4) by adding bismuth, whilst Li et al. [41] increased the service life by the presence of nickel. On the other hand, according to Ding et al. [27], the method of preparation for the same electrode composition also has a great influence on the stability, since the service life tests (100 $mA \cdot cm^{-2}$ in 1 M H_2SO_4) of SnO_2 anodes obtained from electrodeposition reached a higher lifetime (15 h) that those obtained for the electrodes prepared from dip-coating (10 min). From these results, it is inferred that the ceramic electrodes of the present paper have a greatly improved stability in relation to other SnO_2 electrodes.

3.2 Comparison of the electrochemical reactor and electrodes

Figure 3 shows the evolution of the relative Atenolol concentration versus time (t) and applied charge per unit volume (Q) at different current densities for both electrodes and both reactors. On the one hand, for the undivided reactor (Figure 3a and 3b), it can be observed that the rate of ATL depletion increases with the applied current density and is almost independent of the anode type. The ATL was completely degraded at 150 min for an applied current of 83 $mA \cdot cm^{-2}$ and at 210 min for 50 $mA \cdot cm^{-2}$. For the lowest current density, a degradation of 95.5% and 90.5% was achieved with the BDD electrode and the ceramic electrode, respectively. If the evolution of the ATL is represented as a function of the applied charge (Q) (Figure 3b), an overlap of the curves is obtained regardless of the electrode and applied current density. This fact indicates that the same charge is required to remove the same percentage of this organics [42] regardless of whether the anode is BDD or Sb-doped SnO_2 on a ceramic basis.

On the other hand, for the divided reactor, the anode type has a strong influence on the results, as observed in Figure 3c and 3d. In this case, the BDD electrode degraded more ATL than the ceramic one in both graphs. In addition, it was again obtained that the higher the applied current, the greater the degradation velocity of the ATL for both electrodes. For the BDD electrode, the ATL was completely removed at 120, 60 and 40 min for the corresponding current densities of 33, 50 and 83 $mA \cdot cm^{-2}$. In the case of the ceramic electrode, for 50 and 83 $mA \cdot cm^{-2}$, the atenolol was completely eliminated at 150 and 120 minutes respectively, whereas for the lowest applied current value the degradation achieved at the end of the electrolysis was 95%. Figure 3d shows that although the curves were similar for each electrode as the processes were under mass transport control in both

cases, the degradation was faster for the BDD electrode. This was due to the fact that the BDD electrode generated more oxidizing species, as persulfates, hydrogen peroxide and sulfate radicals (Equations from 8 to 11), in addition to the hydroxyl radicals. This trend was not observed in the undivided reactor (Figure 3Figure 3b) because these oxidizing species electrogenerated could be reduced at the cathode according to Equation (12). To verify this statement, iodometry tests were performed (Table 1), and it was demonstrated that the BDD electrode produced more persulfates than the ceramic one and this difference was more noticeable in the divided reactor. The presence of hydrogen peroxide was not observed, and radicals cannot be measured by this technique due to their low lifetime, as previously mentioned.

$$H_2O \rightarrow {}^{\bullet}OH + H^+ + e^- \quad (8)$$

$$2({}^{\bullet}OH) \rightarrow H_2O_2 \quad (9)$$

$$2SO_4^{2-} \rightarrow S_2O_8^{2-} + 2e^- \quad (10)$$

$$SO_4^{2-} \rightarrow SO_4^{-\bullet} + e^- \quad (11)$$

$$S_2O_8^{2-} + 2e^- \rightarrow 2SO_4^{2-} \quad (12)$$

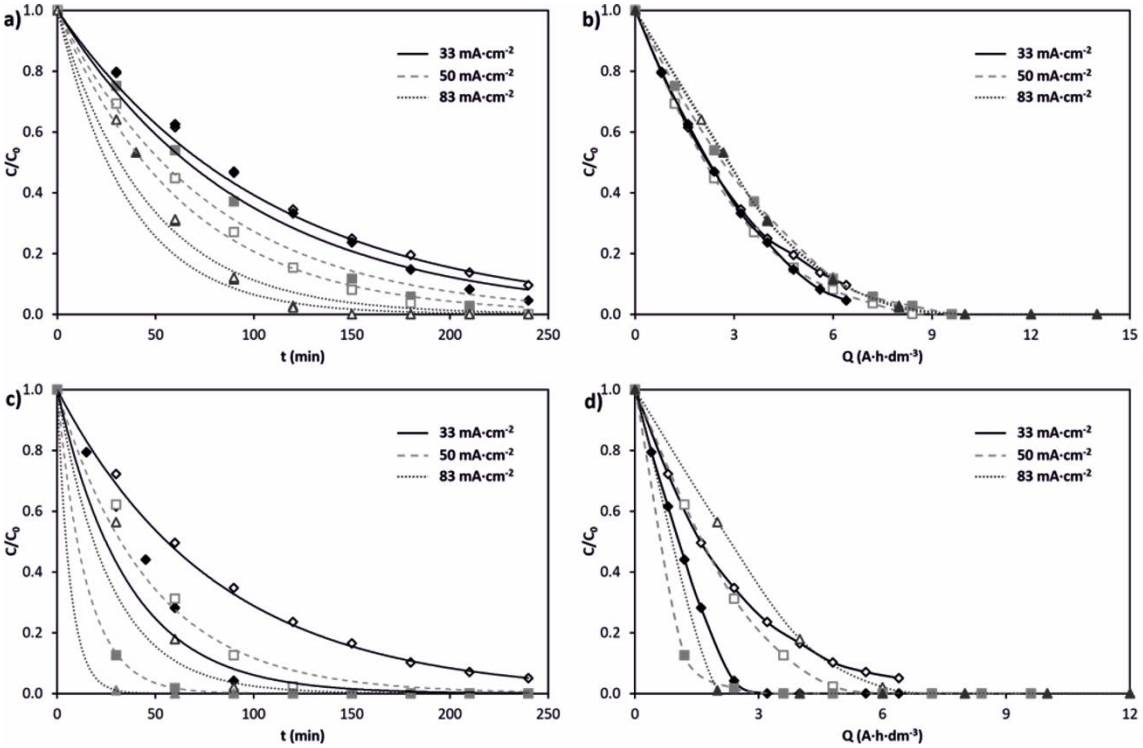

Figure 3. Evolution of the relative concentration of ATL as a function of time (t) and applied charge per unit volume (Q) for the undivided reactor (a and b) and the divided reactor (c and d) at different current densities. Solid points represent BDD electrode and empty points the ceramic electrode.

In addition, from Figure 3 it is inferred that a greater degradation of ATL was achieved in the divided reactor since the membrane prevented the reduction of the intermediate products, and also due to the resulting acid pH value which enhances electro-oxidation. The exponential decrease of the relative ATL concentration observed for both reactors corroborates that the electrochemical system was controlled by mass transport with a typical process of pseudo-first-order. This trend was already observed for the degradation of other organic compounds such as Norfloxacin under the same experimental conditions [16]. Therefore, the velocity of the ATL electro-oxidation reaction can be written as follows:

$$r = -{}^{dC}/_{dt} = k \cdot [^{\bullet}OH] \cdot [ATL] \quad (13)$$

where k is the kinetic constant, [•OH] and [ATL] correspond to the concentration of hydroxyl radicals and Atenolol, respectively, and r is the reaction rate. For a given current density, the concentration of hydroxyl radicals is constant, resulting the velocity equation [43,44]:

$$r = -{}^{dC}/_{dt} = k_{app} \cdot [ATL] \quad (14)$$

where k_{app} is the apparent kinetic constant (k·[•OH]).

The decay of the relative ATL concentration with respect to the degradation time can be calculated by integrating the previous equation as follows:

$$\ln \frac{C_0}{C} = k_{app} \cdot t \quad (15)$$

This equation allows the calculation of the apparent kinetic constants (k_{app}), which are represented as a function of the current density for both types of reactor and electrodes in Figure 4. As can be seen, a linear trend of k_{app} with the current density was observed for all conditions. This fact indicates that the formation of •OH and other oxidizing species, which reacts with ATL, were proportional to the applied current density for all cases. In the membrane reactor, higher k_{app} values were reached since the oxidizing agents and oxidized species could not be reduced at the cathode, therefore the degradation of the ATL was faster in this

reactor. In this figure it was verified again that no significant difference was observed between both electrodes in the undivided reactor. By contrast, in the divided reactor, a dependency with the anodic material was observed, since the BDD presented a higher ATL degradation rate than the ceramic electrode under the same conditions because more oxidants were generated as previously mentioned.

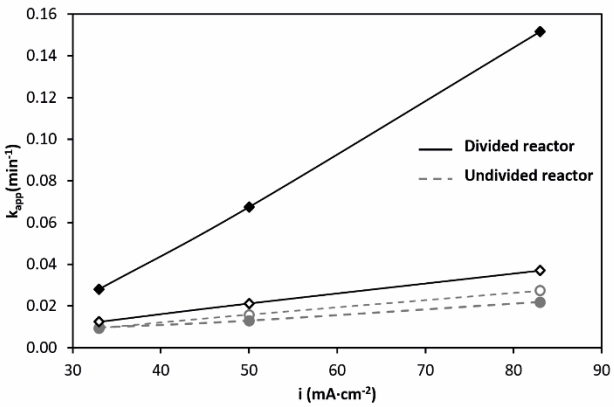

Figure 4. Evolution of apparent kinetic constant (k_{app}) as a function of the applied current density for both types of reactor and electrode. Solid points represent BDD electrode and empty points the ceramic electrode.

Figure 5 presents the relative decrease of the Total Organic Carbon (TOC) as a function of the applied current density for each electrode. This figure highlights a faster decrease of TOC at higher current density with the BDD electrode. The faster TOC removal with time when the current density increase can be explained by the promotion of $^{\bullet}OH$ production thus accelerating the oxidation of organic compounds. For the undivided reactor (Figure 5a), and a time value of 90 minutes, the BDD electrode achieved a mineralization percentage of 34.7%, 50,4% and 64% for the current densities of 33, 50 and 83 mA·cm^{-2}, respectively.

However, for the same conditions but with the ceramic electrode the mineralization degree reached was 23.3%, 27.3% and 43.9%. When the divided reactor was employed (Figure 5b), comparing also the results for the different current densities at 90 minutes, with the BDD electrode it was possible to eliminate 53.5%, 75.6% and 91% of TOC while with the ceramic electrode the corresponding values were 34%, 39.2% and 52.73%, respectively. Therefore, the highest mineralization degree was achieved in the divided reactor, because the membrane avoided the reduction of the electrogenerated oxidizing agents in the cathode, especially with the BDD electrode due to its greater capacity to generate oxidizing agents. In addition, TOC measurements were carried out in the catholyte, and the results showed the non-presence of organic matter in this compartment, so there was no migration of organic by-products through the cationic membrane.

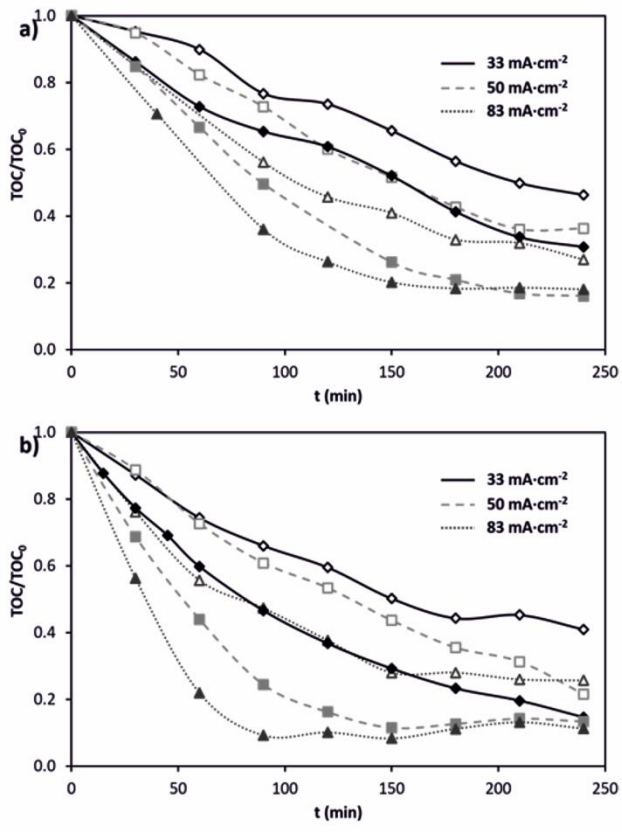

Figure 5. Evolution of the relative concentration of TOC as a function of time in absence (a) and presence (b) of the cation-exchange membrane at different current densities. Solid points represent BDD electrode and empty points the ceramic electrode.

The measured pH of the initial solution was around 7 and remained almost constant during the assays when using the undivided reactor, so the amino group was protonated according to the pK_a value (9.6). However, in the divided one, the pH of the anodic compartment was decreasing with time until reaching an approximate final value of 1, since H^+ ions were formed during the electrochemical process (Equations 7 and 8), and then, they were not directly consumed by the cathodic reactions. The standard redox potential of hydroxyl radicals ($E°(^{\bullet}OH, H^+/H_2O)$) is 2.8 V E [45], and following the Nernst equation for these compounds (Equation 16) [46], at lower pH values the redox potential (E) is greater than at higher values, i.e. at pH=7 the value of E is 2.39 V, while at pH=1 the E is 2.74 V. Therefore, the oxidation reaction was faster in the divided reactor as observed in Figures 3, 4 and 5.

$$E(^{\bullet}OH, H^+/H_2O) = E^0(^{\bullet}OH, H^+/H_2O) - 0.059pH \quad (16)$$

Contrasting the previous figures, it can be inferred that ATL degradation was faster than its mineralization. In order to compare both phenomena, the extent of total electrochemical combustion (Φ) was calculated (Figure 6a and 6b) according to Equation 5. The fact that Φ was less than unity indicates that Atenolol was not directly mineralized to CO_2, but the formation of intermediates

took place, which could also be transformed into CO_2 or other shorter-chain intermediates [47]. As can be observed, Φ rose with the electrolysis time and then, especially for the BDD electrode at higher current densities, Φ values remained practically constant. This last observation means that the organic by-products generated in solution were degrading to CO_2, indicative that the organic matter present was short-chain acids such as formic or oxalic acids [23,48]. The Φ values were also higher at higher i. The trends for both electrodes were the same, although the Φ values for the ceramic electrodes were slightly lower due to the lower amount of oxidizing species generated. The higher values of Φ obtained in the divided reactor were due to the cation-exchange membrane which prevented the oxidized products from being reduced, as previously commented.

Regarding the mineralization current efficiency (Figures 6c and 6d), this parameter was greater for the divided reactor for both electrodes since for this reactor it was possible to eliminate more organic matter. In addition, the electrode that presented better values of MCE was the BDD one. This fact was due to the interaction of the $^{\bullet}OH$ radicals with the surface of each type of electrode [16]. In all cases, MCE values were low but these values are typical of these kind of processes [49,50]. In the undivided reactor (Figure 6c), this parameter remained practically constant with the time, for this reason in Figure 3b the curves were overlapped. For the divided one, it can also be observed that the MCE value decreased with time. This fact was due to the decrease of organic matter in the reactor and the increase of parasitic reactions.

Comparing the MCE values with the applied current density, it is observed that at lower current density the MCE was higher. This may be due to the increase of parasitic reactions such as the formation of O_2 at higher values of applied current density (Equations 2 and 3) and the medium oxidation (Equations from 8 to 11) [51–54].

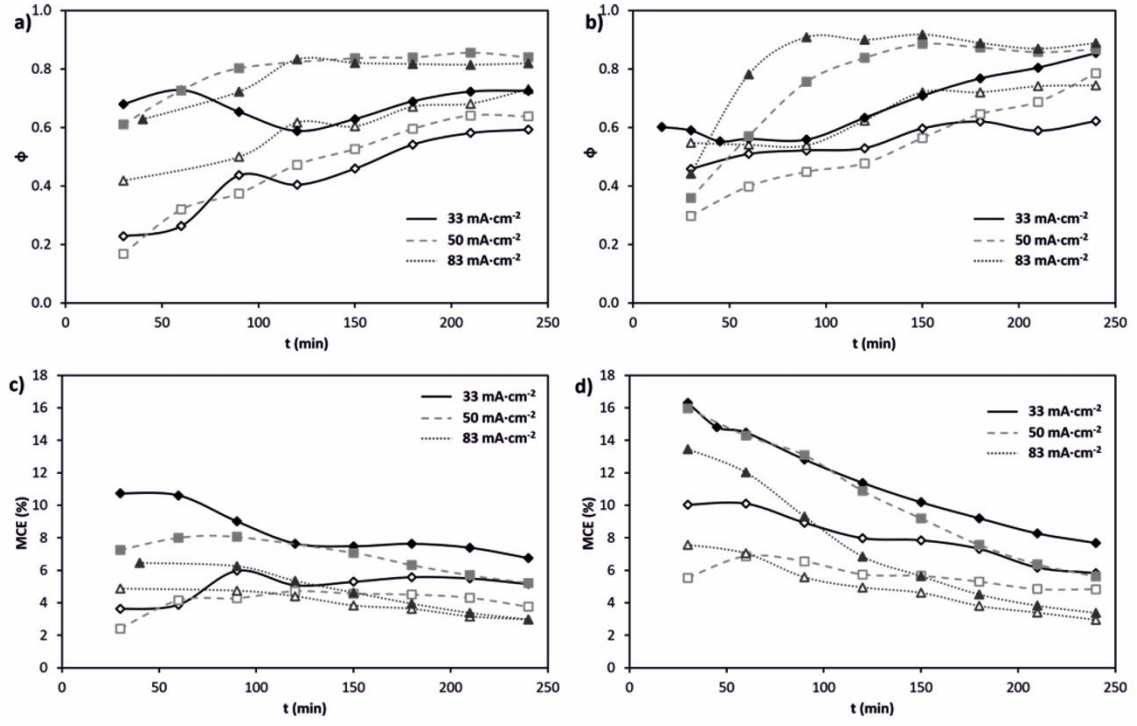

Figure 6. Variation of the extent of total electrochemical combustion (Φ) and the mineralization current efficiency (MCE) as a function of electrolysis time in absence (a and c) and presence (b and d) of the cation-exchange membrane at different current densities. Solid points represent the BDD electrode and empty points the ceramic one.

Regarding the measurements of the inorganic nitrogen ions at the end of the electrolysis, the BDD electrode reached a higher percentage of total nitrogen released from the ATL molecule than the ceramic one. Ions chromatograms

revealed the formation of ammonium and nitrate ions; however, nitrite ion concentration was negligible. The tendency to form NO_3^- and NH_4^+ depended on several factors: the applied current density, electrolysis time, type of electrode and reactor configuration. According to the literature [55], greater tendency to form NO_3^- was observed at higher current density, while at lower current density, the formation of NH_4^+ was favoured. In relation to the electrolysis time, at the beginning of the test a greater formation of ammonium ions was observed, but over time the formation of NO_3^- was greater. As regards the type of electrode, at the end of the electrolysis, with the ceramic electrode more NH_4^+ were formed, on the contrary using the BDD as anode, more NO_3^- were released.

Figure 7 shows the evolution of the percentage of total nitrogen released in the form of NH_4^+ or NO_3^- during the electro-oxidation of ATL at 50 mA·cm^{-2} in (a) absence and (b) presence of cationic membrane with the same electrode (BDD). For both reactor configurations a decrease in the percentage of NH_4^+ formed was observed, while the percentage of NO_3^- ions was increasing. This fact was most notable in the undivided reactor since the NH_4^+ ions was also oxidized to NO_3^-, on the contrary in the divided reactor the NH_4^+ ions passed through the cationic membrane thus preventing their oxidation to NO_3^- (Figure 7b).

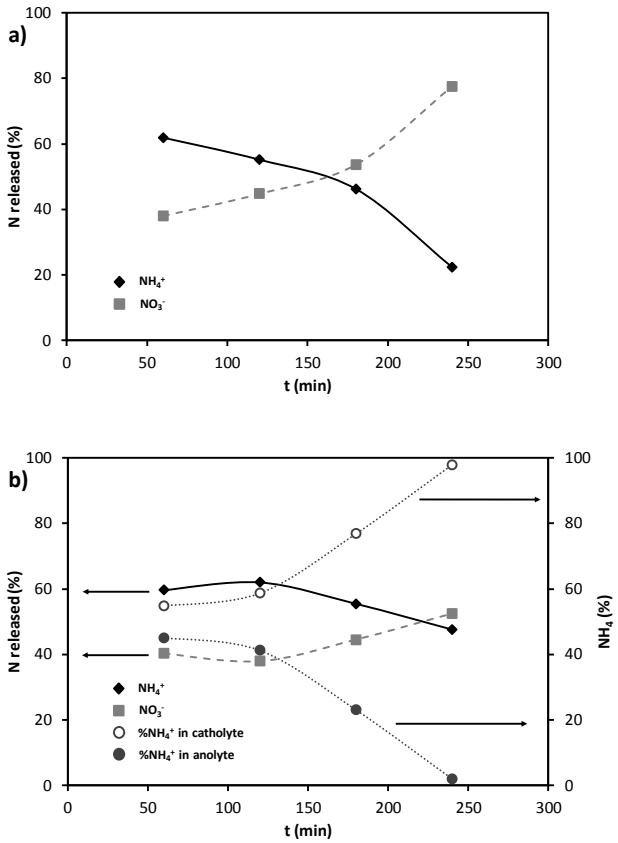

Figure 7. Evolution of the percentage of total nitrogen released in the form of NH_4^+ or NO_3^- as a function of time for (a) undivided and (b) divided reactor at 50 $mA \cdot cm^{-2}$ using BDD electrode.

3.3 Influence of the supporting electrolyte concentration

In order to study whether the concentration of sodium sulfate influences the oxidation process, tests with different concentrations of Na_2SO_4 were carried out in the undivided reactor. Figure 8, which shows the relative TOC decrease with time (t) as a function of the supporting electrolyte concentration for the BDD (a) and the ceramic electrodes (b), presents a different trend according to the type of electrode under study. For the BDD electrode, at a higher concentration of Na_2SO_4 (0.1 M) the mineralization rate was higher, and this difference was more

notable at lower current densities. For example, working at 33 $mA \cdot cm^{-2}$, the TOC removal percentages at the end of the test were 69.3%, 77.1% and 85.46% for the Na_2SO_4 concentrations of 0.014, 0.05 and 0.1 M, respectively. However, for 83 $mA \cdot cm^{-2}$, at the same concentration values of Na_2SO_4 the results were 81.9%, 84.07% and 85.26% of TOC removed. This is due to the fact that BDD also oxidizes the medium to $S_2O_8^{2-}$ and $SO_4^{\bullet-}$ according to Equations 10 and 11, respectively, which present a high oxidation power (2.07 V and 2.4 V vs SHE, respectively) [56,57] and are capable of oxidizing organic matter, increasing the TOC removal. This positive effect had already been observed in other studies [58–60]. Regarding the ceramic electrode for these ranges of sodium sulfate and current density, at higher concentration of supporting electrolyte the mineralization of the ATL was slower. This may be due to either the fact that sulfate ions of higher concentrations could block the active sites of the electrode surface or to the enhancement of the parasitic reactions as was also observed in other studies [61].

The evolution of the apparent kinetic constant as a function of supporting electrolyte concentration at different applied current densities was also studied (not shown). As shown in Figure 4, when the current density increased, k_{app} was higher due to the increase in the formation of oxidizing species. Regarding the type of electrode, for the BDD, an increase in the concentration of sodium sulfate caused an increase in the k_{app}. This fact is due to a greater formation of $S_2O_8^{2-}$ (Table 1) which also acts as oxidant of the organic compounds, as already mentioned. On the contrary, for the ceramic electrodes an increase in the supporting electrolyte concentration caused a decrease in the k_{app} values.

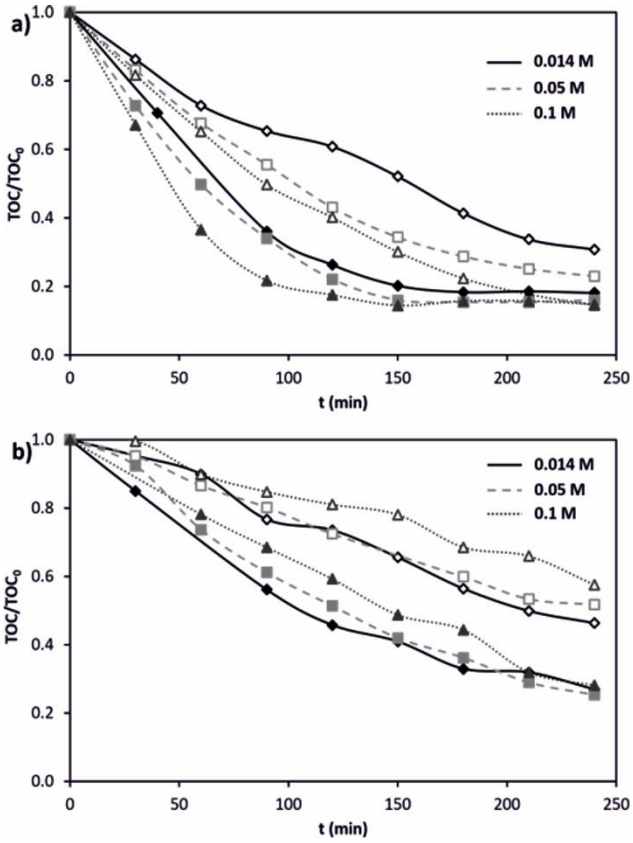

Figure 8. Evolution of the relative concentration of TOC as a function of time for (a) BDD electrode and (b) ceramic electrode at different Na_2SO_4 concentrations in the undivided reactor. Empty points represent 33 $mA \cdot cm^{-2}$ and solid points 83 $mA \cdot cm^{-2}$.

3.4 Toxicity

Biological tests are the most appropriate when measuring the real effects, on the organism being studied, of any physical or chemical agent. In addition, these tests are very diverse, and these effects may occur at different levels, from effects on subcellular structures to effects on whole populations of one type of organism. In

this work, luminescent marine bacteria *Vibrio Fischeri* were used to carry out ecotoxicity tests on the initial and final samples of each test.

Table 1 shows the toxicity values (quantified as toxicity units, TU) for the initial and the final solutions under study for 0.014M of supporting electrolyte (with the two types of reactors and electrodes), and the experiments carried out at 0.1M Na_2SO_4. As can be seen, the initial sample did not show toxicity (TU=0). For the same concentration of supporting electrolyte (0.014M), in the undivided reactor the TU values were zero for both electrodes. On the contrary, in the divided reactor, generally the final solutions showed positive TU values: higher with the applied current and the BDD electrode. As can be seen, the toxicity is directly related to the amount of persulfates formed: if the amount of persulfates present in the solution increases, the toxicity increases.

Figure 9 presents the evolution of the persulfate concentration as a function of the applied current density for both types of reactor and electrode for the lowest supporting electrolyte concentration presented in Table 1 (0.014 M). In the undivided reactor although, the BDD electrode formed persulfates, they were not enough to show toxicity. Comparing the concentration of the supporting electrolyte for the highest applied current density (since more persulfates were generated), the final solution was more toxic at the highest concentration of Na_2SO_4 and using the BDD electrode. According to different studies [62,63], a sample is considered toxic when the TU value is equal to or greater than 10, therefore, any of the tested solutions can be considered toxic.

Table 1. Toxicity units and amount of electrogenerated persulfates for the initial (100 ppm of ATL and 0.014 M of Na_2SO_4) and final solutions of the tests.

Reactor Type	***Anode Material***	***Applied current density(mA·cm^{-2})***	***Persulfates (ppm)***	***Toxicity Units (TU)***
Initial Sample		-	-	0
Undivided	BDD	33.00	96	0
		50.00	115	0
		83.00	153	0
		83.00 (0.1M Na_2SO_4)	630	2
	Ceramic	33.00	0	0
		50.00	0	0
		83.00	10	0
		83.00 (0.1M Na_2SO_4)	230	1
Divided	BDD	33.00	672	3
		50.00	870	3
		83.00	1305	4
	Ceramic	33.00	60	0
		50.00	240	3
		83.00	1017	3

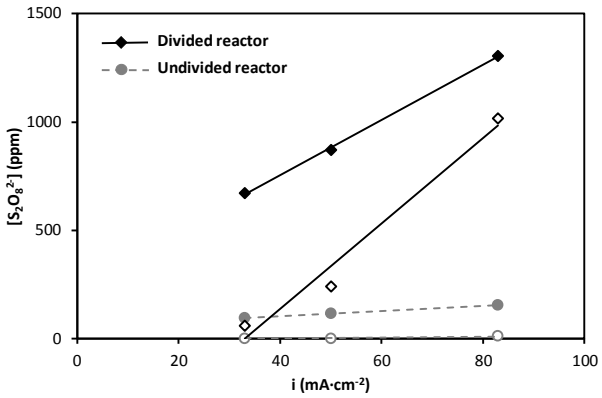

Figure 9. Evolution of the persulfate concentration as a function of the applied current density for both types of reactor and electrode for a solution composed of 100 ppm of ATL and 0.014 M of Na_2SO_4. Solid points represent BDD electrode and empty points the ceramic electrode.

4. Conclusions

New low-cost ceramic electrodes made of tin dioxide doped with antimony have been prepared to carry out EAOPs. The ceramic substrate considerably increased the service lifetime of Sb-doped SnO_2 electrodes.

Experimental results indicate that the electrochemical oxidation is very effective for the complete elimination of Atenolol (ATL). This technique strongly depends on the type of anode used, being the BDD electrode the most efficient due to the low interaction between the hydroxyl radicals (•OH) formed and the electrode surface. The Sb-doped SnO_2 ceramic electrode degrades the organic compound more slowly, but also reaches high values of degradation and mineralization, which demonstrates its viability for this process.

Regarding the type of reactor, the use of a membrane improves the degradation rate of the ATL, the degree of mineralization and the mineralization current efficiency, since it avoids the reduction of the by-products formed during the oxidation and the oxidizing species electrogenerated. In addition, the pH decrease taking place in the anodic compartment of the electrochemical reactor enhances the electro-oxidation kinetics of ATL since the redox potential of the •OH radicals formed in the anode, is greater at lower pHs. Therefore, degradation of the organic compounds takes place faster in the presence of the cation-exchange membrane.

It was also shown that the concentration of sodium sulfate affects the oxidation of ATL for both electrodes. For the BDD electrode, a higher degree of mineralization is achieved with the higher concentration of the supporting electrolyte. On the other hand, the opposite effect occurs for the ceramic electrode.

Finally, regarding the toxicity, it is verified that, although some final solutions were more toxic than the initial one, mainly due to the generation of persulfates, the solutions were not considered toxic in any case, which demonstrates that the electro-oxidation technique is compatible with the environment.

Acknowledgments

The authors thank the financial support from the Ministerio de Economía y Competitividad (Spain) under the project RTI2018-101341-B-C21, co-financed with FEDER funds.

References

[1] M. Gros, M. Petrovic, D. Barceló, Wastewater treatment plants as a pathway for aquatic contamination by pharmaceuticals in the Ebro river basin (northeast spain), Environ. Toxicol. Chem. 26 (2007) 1553–1562. doi:10.1897/06-495R.1.

[2] R. Rosal, A. Rodríguez, J.A. Perdigón-Melón, A. Petre, E. García-Calvo, M.J. Gómez, A. Agüera, A.R. Fernández-Alba, Occurrence of emerging pollutants in urban wastewater and their removal through biological treatment followed by ozonation, Water Res. 44 (2010) 578–588. doi:10.1016/j.watres.2009.07.004.

[3] F.D.L. Leusch, P.A. Neale, C. Arnal, N.H. Aneck-Hahn, P. Balaguer, A. Bruchet, B.I. Escher, M. Esperanza, M. Grimaldi, G. Leroy, M. Scheurer, R. Schlichting, M. Schriks, A. Hebert, Analysis of endocrine activity in drinking water, surface water and treated wastewater from six countries, Water Res. 139 (2018) 10–18. doi:10.1016/j.watres.2018.03.056.

[4] J.R. Domínguez, T. González, P. Palo, J. Sánchez-Martín, M.A. Rodrigo, C. Sáez, Electrochemical degradation of a real pharmaceutical effluent, Water. Air. Soil Pollut. 223 (2012) 2685–2694. doi:10.1007/s11270-011-1059-3.

[5] C.A. Martínez-Huitle, M.A. Rodrigo, I. Sirés, O. Scialdone, Single and Coupled Electrochemical Processes and Reactors for the Abatement of Organic Water Pollutants: A Critical Review, Chem. Rev. 115 (2015) 13362–13407. doi:10.1021/acs.chemrev.5b00361.

[6] S. Garcia-Segura, J.D. Ocon, M.N. Chong, Electrochemical oxidation

remediation of real wastewater effluents — A review, Process Saf. Environ. Prot. 113 (2018) 48–67. doi:10.1016/J.PSEP.2017.09.014.

[7] L.V. de Souza Santos, A.M. Meireles, L.C. Lange, Degradation of antibiotics norfloxacin by Fenton, UV and UV/H2O2, J. Environ. Manage. 154 (2015) 8–12. doi:10.1016/j.jenvman.2015.02.021.

[8] Y.X. Chen, A. Miki, S. Ye, H. Sakai, M. Osawa, Formate, an active intermediate for direct oxidation of methanol on Pt electrode, J. Am. Chem. Soc. 125 (2003) 3680–3681. doi:10.1021/ja029044t.

[9] M. Rueffer, D. Bejan, N.J. Bunce, Graphite: An active or an inactive anode?, Electrochim. Acta. 56 (2011) 2246–2253. doi:10.1016/j.electacta.2010.11.071.

[10] E. Chatzisymeon, A. Dimou, D. Mantzavinos, A. Katsaounis, Electrochemical oxidation of model compounds and olive mill wastewater over DSA electrodes: 1. The case of Ti/IrO2 anode, J. Hazard. Mater. 167 (2009) 268–274. doi:10.1016/J.JHAZMAT.2008.12.117.

[11] C. Comninellis, G. Chen, Electrochemistry for the Environment, Springer, New York, 2010.

[12] Q. Dai, J. Zhou, X. Meng, D. Feng, C. Wu, J. Chen, Electrochemical oxidation of cinnamic acid with Mo modified PbO2 electrode: Electrode characterization, kinetics and degradation pathway, Chem. Eng. J. 289 (2016) 239–246. doi:10.1016/j.cej.2015.12.054.

[13] C. Comninellis, A. Kapalka, S. Malato, S.A. Parsons, I. Poulios, D. Mantzavinos, Advanced oxidation processes for water treatment: advances and trends for R&D, J. Chem. Technol. Biotechnol. 83 (2008) 769–776. doi:10.1002/jctb.

[14] D. Bejan, J.D. Malcolm, L. Morrison, N.J. Bunce, Mechanistic investigation of the conductive ceramic Ebonex® as an anode material, Electrochim. Acta. 54 (2009) 5548–5556. doi:10.1016/j.electacta.2009.04.057.

[15] J. Mora-Gómez, M. García-Gabaldón, E. Ortega, M.-J. Sánchez-Rivera, S. Mestre, V. Pérez-Herranz, Evaluation of new ceramic electrodes based on Sb-doped SnO2 for the removal of emerging compounds present in wastewater, Ceram. Int. 44 (2018) 2216–2222. doi:10.1016/J.CERAMINT.2017.10.178.

[16] J. Mora-Gómez, E. Ortega, S. Mestre, V. Pérez-Herranz, M. García-Gabaldón, Electrochemical degradation of norfloxacin using BDD and new Sb-doped SnO2 ceramic anodes in an electrochemical reactor in the presence and absence of a cation-exchange membrane, Sep. Purif. Technol. 208 (2019) 68–75. doi:10.1016/J.SEPPUR.2018.05.017.

[17] H. Wang, Y. Xiujuan, L. Wu, Q. Wang, D. Sun, A comparative study on electrochemical oxidation of phenol in two types of cells, Russ. J. Electrochem. 41 (2005) 719–724. doi:10.1007/s11175-005-0130-z.

[18] A. El-Ghenymy, F. Centellas, J.A. Garrido, R.M. Rodríguez, I. Sirés, P.L. Cabot, E. Brillas, Decolorization and mineralization of Orange G azo dye solutions by anodic oxidation with a boron-doped diamond anode in divided and undivided tank reactors, Electrochim. Acta. 130 (2014) 568–576. doi:10.1016/j.electacta.2014.03.066.

[19] M. Biel-Maeso, R.M. Baena-Nogueras, C. Corada-Fernández, P.A. Lara-Martín, Occurrence, distribution and environmental risk of pharmaceutically active compounds (PhACs) in coastal and ocean waters

from the Gulf of Cadiz (SW Spain), Sci. Total Environ. 612 (2018) 649–659. doi:10.1016/j.scitotenv.2017.08.279.

[20] J. Hu, X. Jing, L. Zhai, J. Guo, K. Lu, L. Mao, BiOCl facilitated photocatalytic degradation of atenolol from water : Reaction kinetics , pathways and products, Chemosphere. 220 (2019) 77–85. doi:10.1016/j.chemosphere.2018.12.085.

[21] E. Hapeshi, A. Achilleos, M.I. Vasquez, C. Michael, N.P. Xekoukoulotakis, D. Mantzavinos, D. Kassinos, Drugs degrading photocatalytically : Kinetics and mechanisms of ofloxacin and atenolol removal on titania suspensions, Water Res. 44 (2010) 1737–1746. doi:10.1016/j.watres.2009.11.044.

[22] V. Bhatia, G. Malekshoar, A. Dhir, A.K. Ray, Enhanced photocatalytic degradation of atenolol using graphene TiO2 composite, J. Photochem. Photobiol. A Chem. 332 (2017) 182–187. doi:10.1016/j.jphotochem.2016.08.029.

[23] I. Sirés, N. Oturan, M.A. Oturan, Electrochemical degradation of β-blockers. Studies on single and multicomponent synthetic aqueous solutions, Water Res. 44 (2010) 3109–3120. doi:10.1016/j.watres.2010.03.005.

[24] M. Murugananthan, S.S. Latha, G.B. Raju, S. Yoshihara, Role of electrolyte on anodic mineralization of atenolol at boron doped diamond and Pt electrodes, Sep. Purif. Technol. 79 (2011) 56–62. doi:10.1016/j.seppur.2011.03.011.

[25] F. Montilla, E. Morallón, A. De Battisti, J.L. Vázquez, Preparation and Characterization of Antimony-Doped Tin Dioxide Electrodes. Part 1.

Electrochemical Characterization, J. Phys. Chem. B. 108 (2004) 5036–5043. doi:10.1021/jp037480b.

[26] D. Shao, W. Yan, X. Li, H. Yang, H. Xu, A highly stable Ti/TiHx/Sb-SnO2 anode: Preparation, characterization and application, Ind. Eng. Chem. Res. 53 (2014) 3898–3907. doi:10.1021/ie403768f.

[27] H. yang Ding, Y. jie Feng, J. feng Liu, Preparation and properties of Ti/SnO2-Sb2O5 electrodes by electrodeposition, Mater. Lett. 61 (2007) 4920–4923. doi:10.1016/j.matlet.2007.03.073.

[28] Q. Zhuo, S. Deng, B. Yang, J. Huang, G. Yu, Efficient electrochemical oxidation of perfluorooctanoate using a Ti/SnO2-Sb-Bi anode, Environ. Sci. Technol. 45 (2011) 2973–2979. doi:10.1021/es1024542.

[29] D.A.C. Coledam, J.M. Aquino, B.F. Silva, A.J. Silva, R.C. Rocha-Filho, Electrochemical mineralization of norfloxacin using distinct boron-doped diamond anodes in a filter-press reactor, with investigations of toxicity and oxidation by-products, Electrochim. Acta. 213 (2016) 856–864. doi:10.1016/j.electacta.2016.08.003.

[30] D.A.C. Coledam, M.M.S. Pupo, B.F. Silva, A.J. Silva, K.I.B. Eguiluz, G.R. Salazar-Banda, J.M. Aquino, Electrochemical mineralization of cephalexin using a conductive diamond anode: A mechanistic and toxicity investigation, Chemosphere. 168 (2017) 638–647. doi:10.1016/J.CHEMOSPHERE.2016.11.013.

[31] A. El-Ghenymy, C. Arias, P.L. Cabot, F. Centellas, J.A. Garrido, R.M. Rodríguez, E. Brillas, Electrochemical incineration of sulfanilic acid at a boron-doped diamond anode, Chemosphere. 87 (2012) 1126–1133. doi:10.1016/j.chemosphere.2012.02.006.

[32] A. Özcan, Y. Şahin, A.S. Koparal, M.A. Oturan, Propham mineralization in aqueous medium by anodic oxidation using boron-doped diamond anode: Influence of experimental parameters on degradation kinetics and mineralization efficiency, Water Res. 42 (2008) 2889–2898. doi:10.1016/j.watres.2008.02.027.

[33] F.P. Del Greco, F. Kaufman, Lifetime and reactions of OH radicals in discharge-flow systems, Discuss. Faraday Soc. 33 (1962) 128–138. doi:10.1039/DF9623300128.

[34] T. Olmez-Hanci, I. Arslan-Alaton, Comparison of sulfate and hydroxyl radical based advanced oxidation of phenol, Chem. Eng. J. 224 (2013) 10–16. doi:10.1016/j.cej.2012.11.007.

[35] G. Eisenberg, Colorimetric Determination of Hydrogen Peroxide, Ind. Eng. Chem. Anal. Ed. 15 (1943) 327–328. doi:10.1021/i560117a011.

[36] N. Oturan, S. Trajkovska, M.A. Oturan, M. Couderchet, J.-J. Aaron, Study of the toxicity of diuron and its metabolites formed in aqueous medium during application of the electrochemical advanced oxidation process “electro-Fenton,” Chemosphere. 73 (2008) 1550–1556. doi:10.1016/J.CHEMOSPHERE.2008.07.082.

[37] A.N.A. Heberle, S.W. da Silva, C.R. Klauck, J.Z. Ferreira, M.A.S. Rodrigues, A.M. Bernardes, Electrochemical enhanced photocatalysis to the 2,4,6 Tribromophenol flame retardant degradation, J. Catal. 351 (2017) 136–145. doi:10.1016/J.JCAT.2017.04.011.

[38] H.-Y. Ding, Y.-J. Feng, J.-W. Lu, Study on the service life and deactivation mechanism of Ti/SnO2-Sb electrode by physical and electrochemical methods, Russ. J. Electrochem. 46 (2010) 75–79.

doi:10.1134/s1023193510010088.

[39] J. Xue, S. Ma, Q. Bi, Y. Gao, W. Guan, Comparative study on the effects of different structural Ti substrates on the properties of SnO2 electrodes, J. Alloys Compd. 773 (2019) 1040–1047. doi:10.1016/j.jallcom.2018.09.227.

[40] B. Correa-Lozano, C. Comninellis, A. De Battisti, Service life of Ti/SnO2–Sb2O5 anodes, J. Appl. Electrochem. 27 (1997) 970–974. doi:10.1023/A:1018414005000.

[41] X. Li, C. Shao, J. Yu, K. Zhu, Preparation and investigation of nickel-antimony co-doped tin oxide anodes for electro-catalytic oxidation of organic pollutions, Int. J. Electrochem. Sci. 14 (2019) 205–218. doi:10.20964/2019.01.23.

[42] S. Cotillas, E. Lacasa, C. Sáez, P. Cañizares, M.A. Rodrigo, Electrolytic and electro-irradiated technologies for the removal of chloramphenicol in synthetic urine with diamond anodes, Water Res. 128 (2018) 383–392. doi:10.1016/j.watres.2017.10.072.

[43] P. Ghosh, L.K. Thakur, A.N. Samanta, S. Ray, Electro-Fenton treatment of synthetic organic dyes: Influence of operational parameters and kinetic study, Korean J. Chem. Eng. 29 (2012) 1203–1210. doi:10.1007/s11814-012-0011-6.

[44] A.M. Polcaro, S. Palmas, F. Renoldi, M. Mascia, On the performance of Ti/SnO2 and Ti/PbO2 anodes in electrochemical degradation of 2-chlorophenol for wastewater treatment, J. Appl. Electrochem. 29 (1999) 147–151. doi:10.1023/A:1003411906212.

[45] A. Kraft, M. Stadelmann, M. Blaschke, Anodic oxidation with doped

diamond electrodes: A new advanced oxidation process, J. Hazard. Mater. 103 (2003) 247–261. doi:10.1016/j.jhazmat.2003.07.006.

[46] W.H. Koppenol, D.M. Stanbury, P.L. Bounds, Electrode potentials of partially reduced oxygen species, from dioxygen to water, Free Radic. Biol. Med. 49 (2010) 317–322. doi:10.1016/j.freeradbiomed.2010.04.011.

[47] E. Isarain-Chávez, R.M. Rodríguez, P.L. Cabot, F. Centellas, C. Arias, J.A. Garrido, E. Brillas, Degradation of pharmaceutical beta-blockers by electrochemical advanced oxidation processes using a flow plant with a solar compound parabolic collector, Water Res. 45 (2011) 4119–4130. doi:10.1016/J.WATRES.2011.05.026.

[48] E. Isarain-Chávez, C. Arias, P.L. Cabot, F. Centellas, R.M. Rodríguez, J.A. Garrido, E. Brillas, Mineralization of the drug β-blocker atenolol by electro-Fenton and photoelectro-Fenton using an air-diffusion cathode for H2O2 electrogeneration combined with a carbon-felt cathode for Fe2+ regeneration, Appl. Catal. B Environ. 96 (2010) 361–369. doi:10.1016/j.apcatb.2010.02.033.

[49] H. Olvera-Vargas, T. Cocerva, N. Oturan, D. Buisson, M.A. Oturan, Bioelectro-Fenton: A sustainable integrated process for removal of organic pollutants from water: Application to mineralization of metoprolol, J. Hazard. Mater. 319 (2016) 13–23. doi:10.1016/j.jhazmat.2015.12.010.

[50] E. Bocos, N. Oturan, M.Á. Sanromán, M.A. Oturan, Elimination of radiocontrast agent Diatrizoic acid from water by electrochemical advanced oxidation: Kinetics study, mechanism and mineralization pathway, J. Electroanal. Chem. 772 (2016) 1–8. doi:10.1016/j.jelechem.2016.04.011.

[51] S. Velazquez-Peña, C. Sáez, P. Cañizares, I. Linares-Hernández, V. Martínez-Miranda, C. Barrera-Díaz, M.A. Rodrigo, Production of oxidants via electrolysis of carbonate solutions with conductive-diamond anodes, Chem. Eng. J. 230 (2013) 272–278. doi:10.1016/j.cej.2013.06.078.

[52] P. Cañizares, C. Sáez, A. Sánchez-Carretero, M.A. Rodrigo, Synthesis of novel oxidants by electrochemical technology, J. Appl. Electrochem. 39 (2009) 2143–2149. doi:10.1007/s10800-009-9792-7.

[53] A. Kapałka, G. Fóti, C. Comninellis, Kinetic modelling of the electrochemical mineralization of organic pollutants for wastewater treatment, J. Appl. Electrochem. 38 (2008) 7–16. doi:10.1007/s10800-007-9365-6.

[54] C. Flox, P.L. Cabot, F. Centellas, J.A. Garrido, R.M. Rodríguez, C. Arias, E. Brillas, Electrochemical combustion of herbicide mecoprop in aqueous medium using a flow reactor with a boron-doped diamond anode, Chemosphere. 64 (2006) 892–902. doi:10.1016/j.chemosphere.2006.01.050.

[55] S.W. da Silva, J.M. do Prado, A.N.A. Heberle, D.E. Schneider, M.A.S. Rodrigues, A.M. Bernardes, Electrochemical advanced oxidation of Atenolol at Nb/BDD thin film anode, J. Electroanal. Chem. 844 (2019) 27–33. doi:10.1016/j.jelechem.2019.05.011.

[56] C. Liang, C.-F. Huang, N. Mohanty, R.M. Kurakalva, A rapid spectrophotometric determination of persulfate anion in ISCO, Chemosphere. 73 (2008) 1540–1543. doi:10.1016/J.CHEMOSPHERE.2008.08.043.

[57] R.E. Huie, C.L. Clifton, P. Neta, Electron transfer reaction rates and

equilibria of the carbonate and sulfate radical anions, Int. J. Radiat. Appl. Instrumentation. Part C. Radiat. Phys. Chem. 38 (1991) 477–481. doi:10.1016/1359-0197(91)90065-A.

[58] P. Ma, H. Ma, S. Sabatino, A. Galia, O. Scialdone, Electrochemical treatment of real wastewater. Part 1: Effluents with low conductivity, Chem. Eng. J. 336 (2018) 133–140. doi:10.1016/J.CEJ.2017.11.046.

[59] J. Carrillo-Abad, V. Pérez-Herranz, A. Urtiaga, Electrochemical oxidation of 6:2 fluorotelomer sulfonic acid (6:2 FTSA) on BDD: electrode characterization and mechanistic investigation, J. Appl. Electrochem. 48 (2018) 589–596. doi:10.1007/s10800-018-1180-8.

[60] A. Urtiaga, A. Soriano, J. Carrillo-Abad, BDD anodic treatment of 6:2 fluorotelomer sulfonate (6:2 FTSA). Evaluation of operating variables and by-product formation, Chemosphere. 201 (2018) 571–577. doi:10.1016/j.chemosphere.2018.03.027.

[61] C. Zhang, X. Du, Z. Zhang, D. Fu, The peculiar roles of sulfate electrolytes in BDD anode cells, J. Electrochem. Soc. 162 (2015) E85–E89.

[62] R. Boluda, J.F. Quintanilla, J.A. Bonilla, E. Sáez, M. Gamón, Application of the Microtox® test and pollution indices to the study of water toxicity in the Albufera Natural Park (Valencia, Spain), Chemosphere. 46 (2002) 355–369. doi:10.1016/S0045-6535(01)00092-3.

[63] J.I. Seco, C. Fernández-Pereira, J. Vale, A study of the leachate toxicity of metal-containing solid wastes using Daphnia magna, Ecotoxicol. Environ. Saf. 56 (2003) 339–350. doi:10.1016/S0147-6513(03)00102-7.